Two-photon luminescence from polar bis-terpyridyl-stilbene derivatives of Ir(III) and Ru(II)†

Louise S. Natrajan,*[a] Anita Toulmin,[a] Alex Chew[a] and Steven W. Magennis*[a,b]

Received 29th June 2010, Accepted 3rd September 2010
DOI: 10.1039/c0dt00750a

Four structurally related iridium(III) and ruthenium(II) complexes bearing two polar terpyridyl–stilbene derived chromophores 4-(4-{2-[4-(methoxy)phenyl]ethenyl}phenyl)-2,2′-6′,2″-terpyridine (ttpyeneanisole) and 4-(4-{2-[phenyl]ethenyl}phenyl)-2,2′-6′,2″-terpyridine (tpystilbene) have been synthesised and characterised in the solid state and in solution. In the solid state, the dihedral angle subtending the pyridyl and tolyl groups of 27.1° in the Ir(III) complex $[Ir(ttpyeneanisole)_2]\cdot 3PF_6$ is more acute than in the Ru(II) derivative $[Ru(tpystilbene)_2]\cdot 2PF_6$ (35.5°), indicating the presence of a greater degree of π-delocalisation across the terpyridine unit in the former compound. Their luminescence properties in fluid solution have been investigated following both resonant and non-resonant excitation. We have shown that each of the complexes undergoes two-photon excitation when excited in the near infrared (740 to 820 nm), with two-photon absorption cross sections in the range $11–67 \times 10^{-50}$ cm^4 s $photon^{-1}$. The larger cross sections for the Ir(III) complexes reflect the differences observed in the solid state. This work therefore demonstrates that such complexes are promising as luminescent markers for 3D imaging and illustrates that simple functionalisation of the chromophores and the choice of metal can lead to marked enhancements in the two-photon cross sections (σ_2) compared to those of simpler heteroleptic polypyridyl based derivatives.

Introduction

Materials that undergo multiphoton excitation,[1] the simultaneous absorption of two or more photons, are finding increasing use in many applications including up-converting lasing,[2] 3D data storage,[3] optical power limiting,[4] microfabrication,[5] 3D fluorescence microscopy,[6] photodynamic therapy[7] and the targeted delivery of bioactive molecules.[8] The multiphoton process is mediated *via* intermediate 'virtual' excited states. The selection rules for one-photon excitation (OPE) and multiphoton excitation may result in different excited states being accessed or, as commonly occurs, the multiphoton absorption of low-energy photons populates the same excited states that are accessible through one-photon absorption.[1] Multiphoton excitation has several advantages over conventional one photon excitation. For imaging applications, the non-linear absorption of a focused laser beam enables 3D control of the excitation process. Furthermore, molecules may undergo multiphoton absorption in the near-infrared region, where many materials (including biological tissue) have low one-photon absorption coefficients, thereby allowing deeper light penetration (typically, up to several hundred μm).[9]

In the case of two-photon excitation (TPE) with a single monochromatic laser source, which accounts for the majority of studies,[1–8] two photons of approximately half the energy of the resonant excited state are absorbed. A quantitative measure for the probability of two-photon absorption (TPA) for a compound is the two-photon absorption cross-section (σ_2),[10] which can be viewed as the two photon equivalent of the one-photon molar absorption coefficient ε. There are a variety of synthetic approaches to increase σ_2 and these tend to be based on increasing the π network conjugation within the framework of a molecule, or the generation of large changes in excited state polarisation following photoexcitation.[11] Large values of σ_2 can arise from centrosymmetric charge transfer and substantial values can be achieved in push–pull electron donor–acceptor (D–A) diads, in D–π–A type assemblies, and variants thereof. These structural motifs have been applied extensively to the construction of organic-based chromophores yielding materials with remarkably high two-photon absorption cross sections.[1] By contrast, far fewer metal-based chromophores have been investigated even though they possess attractive chemical and photophysical properties.[12–16]

Second and third row transition metal oligopyridyl complexes lend themselves particularly well to non-linear processes.[17,18] For instance, the rich photochemistry of the charge transfer excited triplet states of Ir (and Ru) complexes with an N_6 coordination sphere gives rise to long phosphorescent lifetimes in aerated fluid solution in the microsecond time domain.[19] Compounds with long radiative lifetimes offer improved temporal discrimination over organic fluorophores and enable the application of time gating techniques to eliminate short-lived background fluorescence and scattered light.[20] In addition, these complexes are almost optically transparent at wavelengths above 750–800 nm and are kinetically and photochemically robust. Interestingly, cyclometallated Ir(III)

[a]*School of Chemistry, The University of Manchester, Oxford Road, Manchester, UK, M13 9PL. E-mail: louise.natrajan@manchester.ac.uk; Fax: +44 (0)161 275 4616; Tel: +44 (0)161 275 1426*
[b]*Photon Science Institute, The University of Manchester, Oxford Road, Manchester, UK, M13 9PL. E-mail: steven.magennis@manchester.ac.uk; Tel: +44 (0)161 275 1014*

† Electronic supplementary information (ESI) available: Positive electrospray mass spectra of the complexes including calculated isotope patterns and emission and excitation spectra of the uncomplexed ligands in DMSO. CCDC reference numbers 783187 and 783188. For ESI and crystallographic data in CIF or other electronic format see DOI: 10.1039/c0dt00750a

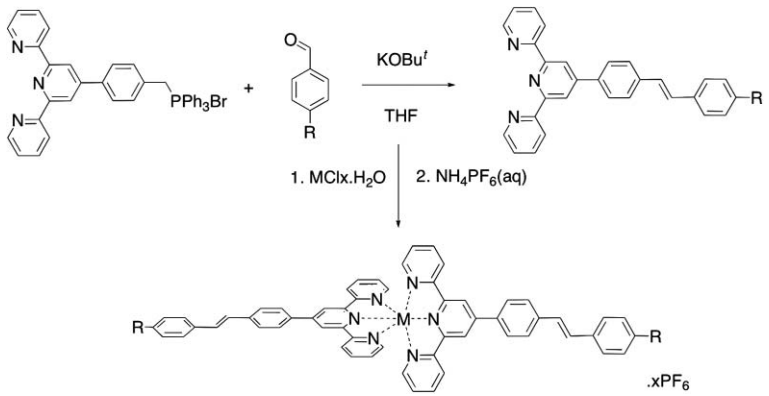

Scheme 1 Synthesis of ligands and complexes; R = H, OMe, M = Ir ($x = 3$), Ru ($x = 2$).

derivatives can exhibit more unusual non-linear optical properties including both TPA and reversible saturated absorption (RSA) and simultaneous one and two-photon phosphorescence.[14]

In this contribution, we report the synthesis, one-photon and two-photon photophysical behaviour of several bis terpyridyl Ir^{3+} and Ru^{2+} complexes. The terpyridine ligands, 4-(4-{2-[4-(methoxy)phenyl]-ethenyl}phenyl)-2,2′-6′,2″-terpyridine (ttpyeneanisole) and 4-(4-{2-[phenyl]ethenyl}phenyl)-2,2′-6′,2″-terpyridine (tpystilbene), have been structurally elaborated by Wittig condensation to afford, when complexed, polar D–π–A–π–D conjugated chromophores with appreciable two-photon absorption cross sections.

Results and Discussion

Synthesis of ligands and complexes

The ligands ttpyeneanisole and tpystilbene and their corresponding iridium and ruthenium complexes were prepared as illustrated in Scheme 1. 4′-(*p*-Tolyl)-2,2′:6′,2″-terpyridine, (ttpy) was prepared in good yield according to a published procedure using the Kröhnke methodology.[21] The tolyl group was then brominated by a free radical reaction using *N*-bromosuccinimide in CCl_4 in the presence of a catalytic amount of benzoyl peroxide initiator whilst irradiating with a UV lamp.[22,17] 4′-(Phenyl-*p*-bromomethyl)-2,-2′:6′,2″-terpyridine was then near quantitatively converted to the phosphonium bromide salt by heating with PPh_3 in toluene.[17] Finally, the Wittig reaction was employed to extend the conjugation of the terpyridine units by reaction of anisaldehyde or benzaldehyde with ttpy phosphonium bromide and KO^{t}Bu in dry THF. After extensive trituration in methanol, the ligands were isolated analytically pure as pale yellow solids in moderate yields (39–49%).

The ruthenium adducts were prepared using standard methodologies[23] and the iridium complexes by modification of the procedures described by Sauvage and Williams[24,25] (Scheme 1) by treatment of the corresponding metal chloride salt with one or two equivalents of the ligands. The complexes were purified by metathesis with NH_4PF_6 and repeated recrystallisation from acetone–ether or acetonitrile–ether. In the case of the complex $[Ir(ttpyeneanisole)_2]\cdot 3PF_6$, this resulted in the precipitation of X-ray quality single crystals whose structure was elucidated by diffraction analysis (Fig. 1).

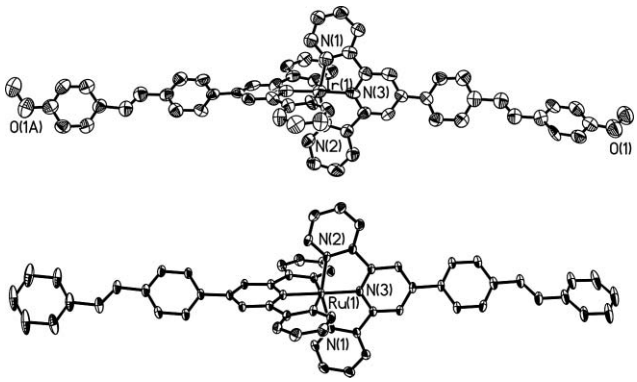

Fig. 1 Thermal ellipsoid drawings of $[Ir(ttpyeneanisole)_2]^{3+}$ (top) and $[Ru(tpystilbene)_2]^{2+}$ (bottom) at the 30% probability level. H atoms, PF_6 counterions and lattice solvent molecules omitted for clarity.

Solid state structure of the complexes. Deep red blocks of $[Ir(ttpyeneanisole)_2]\cdot 3PF_6$ were deposited by layering an acetonitrile solution of the complex with diethyl ether (3 : 1 v:v) whereas red single crystals of $[Ru(tpystilbene)_2]\cdot 2PF_6$ were grown by slow evaporation of a concentrated acetone solution of the complex; selected interatomic distances and angles are given in Table 1. In both structures (Fig. 1), the coordination geometries of the metal cations are distorted from a perfect octahedron evidenced by the terpyridine–metal bite angles and the angles between the two *ortho* pyridine substituents on the central ring. Respectively, these are measured at 159.04° and 103.4 for $[Ru(tpystilbene)_2]\cdot 2PF_6$ and 158.07° and 104.0° in $[Ir(ttpyeneanisole)_2]\cdot 3PF_6$. The metal–nitrogen bond distances in both complexes (range 2.066(3) Å–1.94(2) Å) are unremarkable and as with the bond angles (Table 1),

Table 1 Selected interatomic distances (Å) and angles (deg) for $[Ir(ttpyeneanisole)_2]\cdot 3PF_6$ and $[Ru(tpystilbene)_2]\cdot 2PF_6$

	$[Ir(ttpyeneanisole)_2]\cdot 3PF_6$	$[Ru(tpystilbene)_2]\cdot 2PF_6$
M(1)–N(1)	2.00(2)	2.066(3)
M(1)–N(2)	2.045(19)	2.062(3)
M(1)–N(3)	1.94(2)	1.976(4)
N(3)–M(1)–N(3)′	177.4(11)	178.98(17)
N(3)–M(1)–N(2)′	99.8(8)	100.24(13
N(2)–M(1)–N(2)′	89.6(10)	92.31(19)
N(3)–M(1)–N(1)	80.7(8)	79.03(12)
N(2)–M(1)–N(1)	159.0(9)	158.07(13)
N(1)–M(1)–N(1)′	87.9(12)	92.11(19)

Table 2 One- and two-photon properties of the ligands and complexes

Compound	λ_{abs}/nm	λ_{ex}/nm[d]	λ_{em}/nm	τ_{MeCN}/ns[a]	τ_{MeOH}/ns[a]	Φ_{MeCN}[b]	σ_2/GM[c]
tpystilbene[e]	289, 336	405	420	1	[f]	[f]	[f]
ttpyeneanisole[e]	287, 352	405	460	2	[f]	[f]	[f]
$[Ir(tpystilbene)_2]\cdot 3PF_6$	292, 377	405	550	1346	1428	0.0059	67
$[Ir(ttpyeneanisole)_2]\cdot 3PF_6$	323, 434	405	560	1536	1512	0.0026	58
$[Ru(tpystilbene)_2]\cdot 2PF_6$	312, 496	405	540	2	2	0.0059	12
$[Ru(ttpyeneanisole)_2]\cdot 2PF_6$	310, 497	405	600	3	3	0.0029	11

[a] Lifetimes quoted at 405 nm excitation using a 550 –650 nm bandpass interference filter and are subject to ± 10% error. [b] Quantum yields determined relative to quinine sulfate in 1M H_2SO_4 at 350 nm excitation, $\phi = 0.58$; estimated error ± 20%. [c] Two-photon cross section, σ_2, at 740 nm, GM = 10^{-50} cm^4 s $photon^{-1}$; estimated error ± 30%. [d] Identical results within error were determined at 375 nm excitation. [e] Measurements performed in DMSO. [f] Value not measured.

are within the range of those previously reported for mono and bis-terpyridyl Ir and Ru complexes.[25,26] More pertinent to the photophysical properties of the complexes, it is interesting to note that the pyridyl and phenyl rings are not mutually co-planar and are twisted considerably out of the plane of the chelating terpyridine unit. This twist is more pronounced in the $[Ru(tpystilbene)_2]^{2+}$ cation, where the dihedral angle between the central pyridyl ring and the tolyl group is 35.5° and that between the tolyl and phenyl substituent is 28.4°. In the solid state structure of $[Ir(ttpyeneanisole)_2]\cdot 3PF_6$ however, the pyridyl–tolyl dihedral angle of 27.1° is considerably more acute possibly reflecting a greater degree of π-delocalisation across the ttpy unit, whereas the twist angle between the tolyl and the phenyl ring bearing the methoxy substituent has opened up to 37.6°.

Photophysical properties

One-photon absorption and emission properties. The ground state electronic absorption spectra of the complexes were recorded in acetonitrile solutions; the principle absorption maxima are listed in Table 2 and the spectra are shown in Fig. 2. The spectra of all the complexes display several intense broad transitions in the UV region (between 200 and 350 nm) which are assigned to spin allowed ligand centred (LC) $^1\pi$–π^* transitions by comparison with related aryl modified terpyridyl Ir^{3+} and Ru^{2+} complexes.[25–27] In the Ru^{2+} complexes, these transitions are red shifted when compared to the parent complexes $[Ru(tpy)_2]^{2+}$ and $[Ru(ttpy)_2]^{2+}$ and tail into the visible region owing to the increased conjugation upon introduction of the pendent alkene and aromatic groups. The ^{1}MLCT absorption bands are observed at lower energy (~ 497 nm) and are also located at longer wavelength than the bis terpyridine and tolyl-terpyridine Ru(II) adducts (476 and 487 nm respectively). In addition to the more localised ligand-centered UV transitions, the Ir^{3+} complex $[Ir(ttpyeneanisole)_2]\cdot 3PF_6$ also displays an intense broad absorption band at 434 nm. This visible absorption is attributed to an intraligand charge transfer (ILCT) transition, which is likely to be ^1n-π^* in origin; the anisole group acting as the electron donor and the coordinated terpyridine unit as the electron acceptor. By contrast, this absorption feature in the stilbene analogue $[Ir(tpystilbene)_2]\cdot 3PF_6$ is observed at much higher energy (377 nm) and by the very nature of the ligand, must be $^1\pi$–π^* in character. Although in these homoleptic complexes there is no permanent dipole moment in the ground state, the ILCT absorption band in $[Ir(ttpyeneanisole)_2]\cdot 3PF_6$ undergoes a more pronounced solvatochromic shift in MeOH (445 nm) than

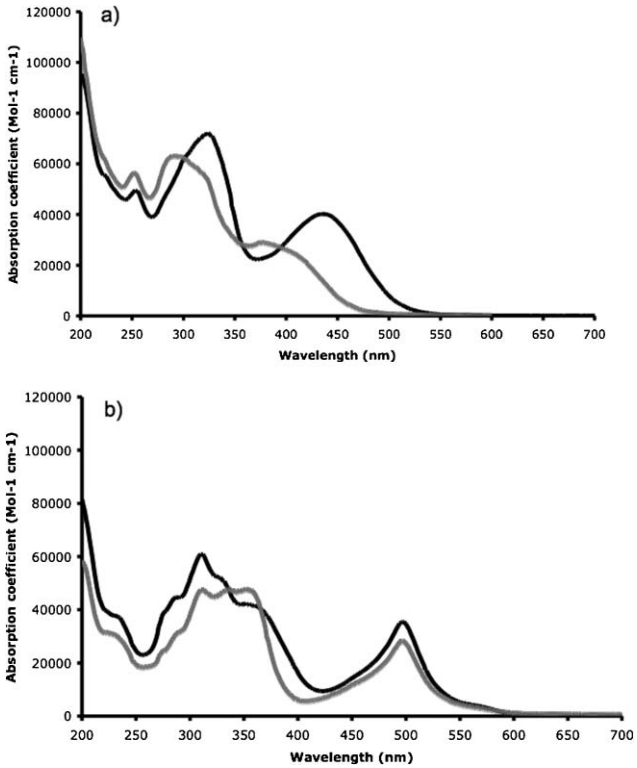

Fig. 2 UV–vis absorption spectra of a) $[Ir(ttpyeneanisole)_2]\cdot 3PF_6$ (black trace) and $[Ir(tpystilbene)_2]\cdot 3PF_6$ (grey trace), b) $[Ru(ttpyeneanisole)_2]\cdot 2PF_6$ (black trace) and $[Ru(tpystilbene)_2]\cdot 2PF_6$ (grey trace) in MeCN.

the LC transitions which essentially remain the same as those recorded in MeCN solution (324 nm). This shift to lower energy in the more polar solvent is suggestive of a more polar excited state and confirms the higher degree of charge separation in this transition.

Unlike its cyclometallated counterpart ($Ir(ppy)_3$) whose luminescence involves a substantial contribution from the ^{3}MLCT excited state, the photoluminescence from simple $[Ir(tpy)_2]^{3+}$ derivatives is longer lived and has been shown to originate from ligand-based triplet transitions, primarily of $^3\pi$–π^* character.[25] Earlier work has shown that the lifetime of this excited state can be elongated by introduction of simple aryl substituents at the 4′ position of the central terpyridine ring. In aerated, fluid MeCN solution at room temperature, the Ir^{3+} complexes $[Ir(ttpyeneanisole)_2]\cdot 3PF_6$ and $[Ir(tpystilbene)_2]\cdot 3PF_6$ are both strongly photoemissive when excited into the UV–vis absorption

bands (250–450 nm); they display broad featureless emission bands centered at *ca.* 550 nm (Fig. 3). The absence of vibrationally resolved features in these spectra observed in the unsubtituted $[Ir(tpy)_2]^{3+}$ derivative[24] and the fact the emission is red shifted by *ca.* 100 nm with respect to the parent tpy compound reflects the considerably higher degree of conjugation in the excited states and possible co-involvement of close lying ^{3}MLCT and lower lying ^{3}ILCT excited states. The fact that the emission bands are somewhat broadened also suggests that a range of conformers differing in dihedral angles between the terpyridyl and pendent aryl groups exist in fluid solution at room temperature. Interestingly, the excitation spectra (monitored at the emission maxima of 550 nm, Fig. 3) for both the Ir^{3+} compounds in question do not correspond well to the absorption spectra, indicating that different excited states result in the observed emission profile. The bands in the excitation spectra are blue shifted with respect to those in the absorption spectra, but follow the same general form giving further weight to the argument that excited state mixing between the LC, MLCT and π–π^* ILCT levels may be responsible for the emission. However, whether the relative contribution of metal based orbitals in this CT emission is significant remains unclear. For comparison, in the complex $[Ir(tpy\text{-}\phi\text{-}NMe_2)_2]^{3+}$, the lowest excited state has been attributed to a ^3n-π^* state and that in $[Ir(tpy)(tpy\text{-}\phi\text{-}Ph)]^{3+}$ is thought to be predominantly CT in origin.[25]

The emission is independent of excitation wavelength in accordance with Kasha's law and the radiative lifetimes in air equilibrated MeCN follow monoexponential decay kinetics and are 1.54 μs and 1.35 μs for $[Ir(ttpyeneanisole)_2]\cdot 3PF_6$ and $[Ir(tpystilbene)_2]\cdot 3PF_6$ respectively. Similar values are recorded in methanol solution. These lifetimes are significantly longer than in $[Ir(tpy)_2]^{2+}$ itself (1.0 μs)[25] but are shorter than that measured for the tolyl-substituted derivative which has a radiative lifetime of 2.4 μs in MeCN. This significant decrease in lifetime may also imply involvement of the ^{3}MLCT level in the emissive state, since shorter lifetimes are often observed in these systems in aerated media.[25] In addition, the potential for triplet metal-centered (^{3}MC) states to contribute to non radiative quenching of the emissive state cannot be ruled out.

In contrast to Ir^{3+} terpyridine complexes, the Ru^{2+} counterparts are, in general, only weakly emissive from their ^{3}MLCT states ($\tau_{MLCT} \leq 1$ ns) at room temperature; this is because the lower lying ^{3}MC states are thermally accessible from the ^{3}MLCT excited states which provides a rather efficient pathway for non-radiative energy loss in fluid solution.[28] However, the Ru^{2+} derivatives of ttpyeneanisole and tpystilbene display no emission that is metal based in character, but rather exhibit short lived (2–3 ns) visible emission, which is a superposition of two features. This emission is likely to be ligand based fluorescence and phosphorescence which originates from the ligand excited states as inferred from examination of the excitation spectra (Fig. 4) and excitation and emission spectra of the uncomplexed ligands.†

The quantum yields of emission in aerated MeCN (Table 1) of all the complexes are less than 1% but are of a similar magnitude to compounds such as $[Ir(tpy)(tpy\text{-}\phi\text{-}Ph)]^{3+}$, $[Ir(tpy\text{-}\phi\text{-}Ph)_2]^{3+}$ and $[Ir(tpy\text{-mesityl})_2]^{3+}$ whose quantum yields were determined in degassed solutions where triplet oxygen annihilation is negligible.[25]

Two-photon absorption and emission properties. To investigate whether these complexes could be excited by a multiphoton

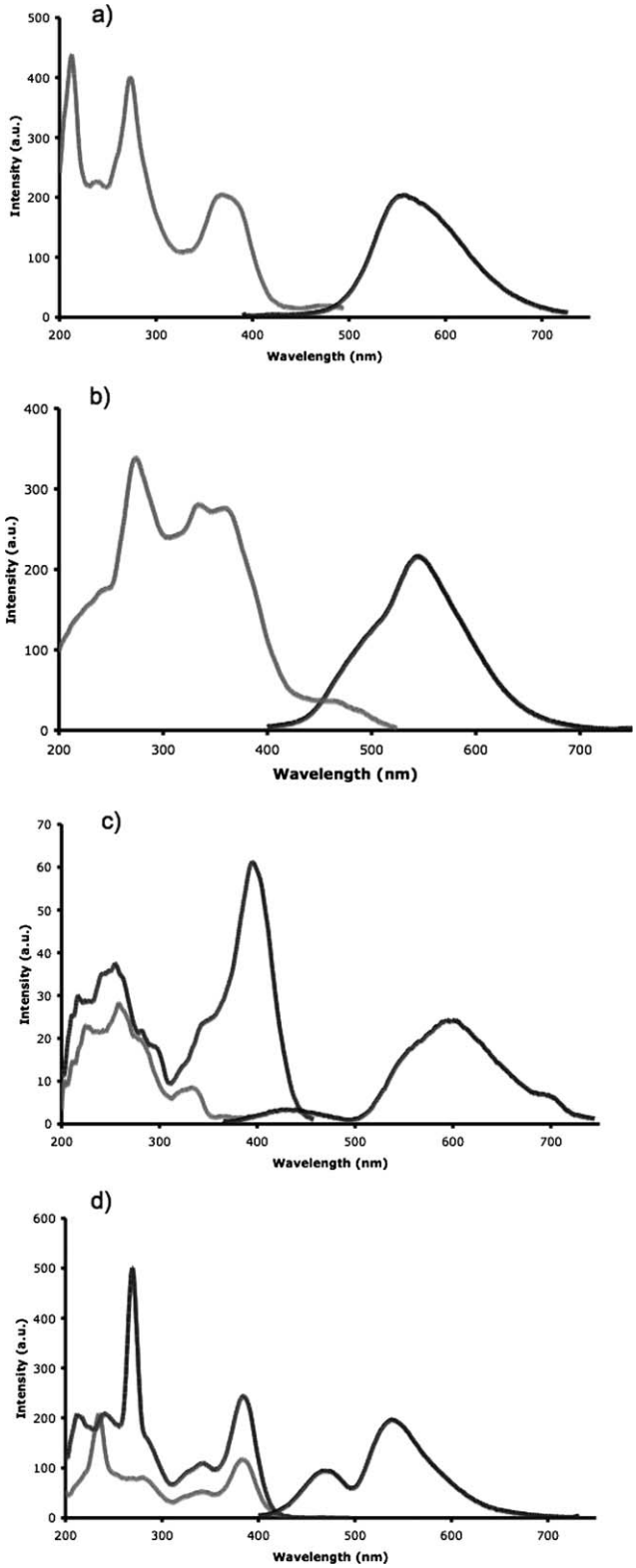

Fig. 3 Corrected steady state emission (black traces) and excitation spectra (grey traces) of a) $[Ir(ttpyeneanisole)_2]\cdot 3PF_6$, b) $[Ir(tpystilbene)_2]\cdot 3PF_6$, c) $[Ru(ttpyeneanisole)_2]\cdot 2PF_6$ (dark grey trace, excitation spectrum monitored at 550 nm emission and light grey trace, excitation spectrum monitored at 450 nm emission) and d) $[Ru(tpystilbene)_2]\cdot 2PF_6$ (dark grey trace, excitation spectrum monitored at 550 nm emission and light grey trace, excitation spectrum monitored at 450 nm emission) recorded at 350 nm excitation in MeCN.

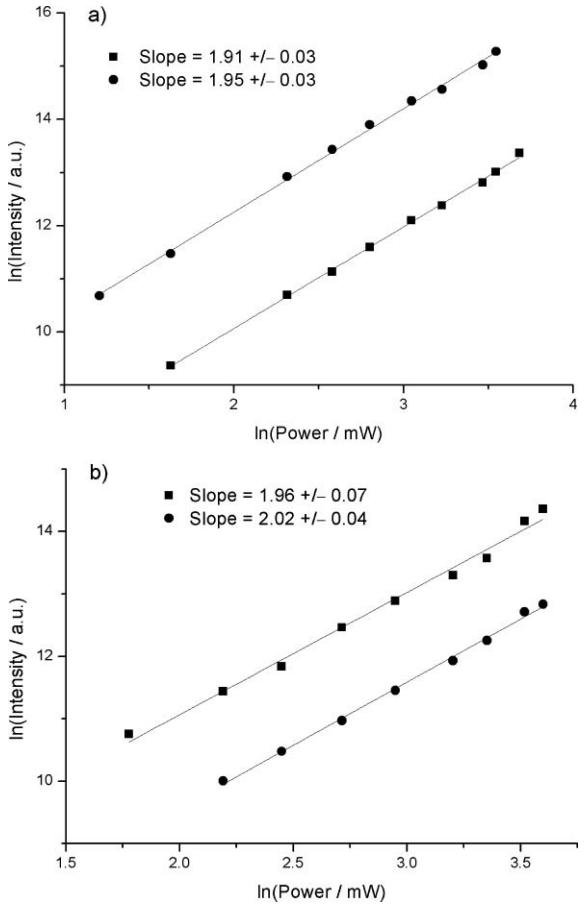

Fig. 4 Dependence of luminescence intensity on excitation power following non-resonant excitation at 740 nm a) $[Ir(ttpyeneanisole)_2]\cdot 3PF_6$ (■) and $[Ir(tpystilbene)_2]\cdot 3PF_6$ (●) b) $[Ru(ttpyeneanisole)_2]\cdot 2PF_6$ (●) $[Ru(tpystilbene)_2]\cdot 2PF_6$ (■) in MeCN. The solid line shows the best straight line fit to the data ($R = 99.9\%$).

process, solutions were irradiated with an ultrafast titanium sapphire laser. The complexes had negligible one-photon absorption at the near infrared excitation wavelengths. Luminescence, with the same broad spectrum that was observed upon resonant excitation, was detected from MeCN solutions of the complexes. Operating the laser in continuous wave mode, but with the same average power, resulted in no detected luminescence. The luminescence intensity was studied as a function of excitation power, which demonstrated that a two-photon excitation mechanism is operating for all four complexes. Fig. 4 shows the results of the power dependence measurements with an excitation wavelength of 740 nm; the slope of the logarithmic plots is 2 within experimental error, which is strong evidence that a two-photon process is occurring. Similar results were obtained for excitation at 800 nm.

To assess the efficiency of the two-photon process, the two-photon cross-section (σ_2), the luminescence intensity of each complex was compared to that of a reference compound, rhodamine B in methanol, for which the two-photon cross section is known.[10] The results for excitation at 740 nm are shown in Table 1. The Ru(II) complexes have similar cross sections, 11 and 12 GM for $[Ru(ttpyeneanisole)_2]\cdot 2PF_6$ and $[Ru(tpystilbene)_2]\cdot 2PF_6$, respectively. The cross sections of the Ir(III) complexes (58 and 67 GM for $[Ir(ttpyeneanisole)_2]\cdot 3PF_6$ and $[Ir(tpystilbene)_2]\cdot 3PF_6$, respectively) are similar to each other but approximately six times larger than for the Ru(II) analogues. In comparison, the one-photon extinction coefficients at 370 nm for all four complexes are very similar.

To investigate the origin of the two-photon transition, the cross-section was measured as a function of excitation wavelength from 740–820 nm (Fig. 5). The low resolution of these spectra preclude a detailed analysis, but they suggest that there are a number of distinct spectral transitions that can occur *via* a two-photon process, analogous to the structured one-photon excitation spectra (Fig. 3).

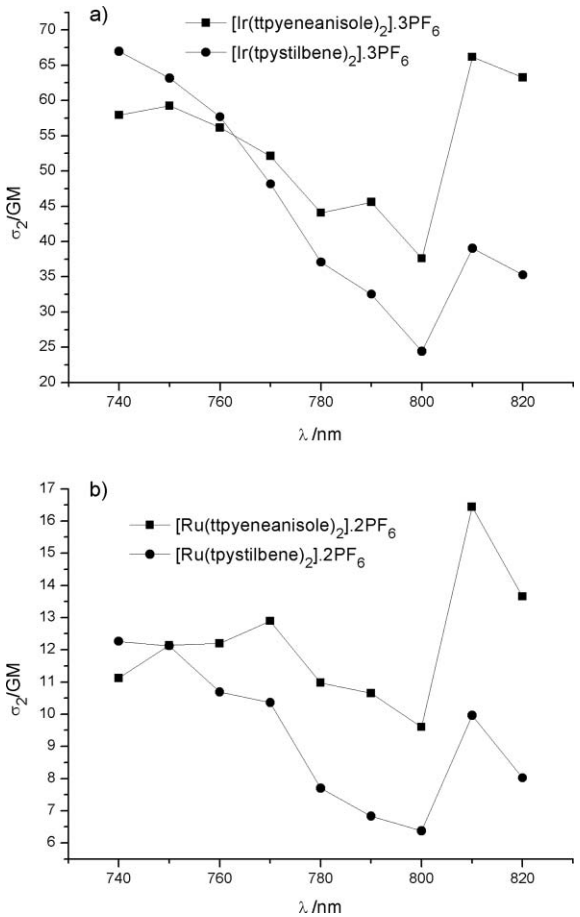

Fig. 5 Two-photon excitation spectra of a) $[Ir(ttpyeneanisole)_2]\cdot 3PF_6$ and $[Ir(tpystilbene)_2]\cdot 3PF_6$, and b) $[Ru(ttpyeneanisole)_2]\cdot 2PF_6$ and $[Ru(tpystilbene)_2]\cdot 2PF_6$ in MeCN. Estimated uncertainties are ± 30%.

The measured two-photon cross sections are considerably larger than many other heteroleptic transition metal polypyridyl and acetylide complexes[12–14] demonstrating that these structures are a good starting point to develop multiphoton-active materials. Of course, for use in 3D luminescence imaging, the emission process must also be efficient. The measured one-photon quantum yields for these complexes are in general, quite low (0.3–0.6%), so developments to optimise this aspect should proceed in parallel with attempts to improve the cross sections; it is however worth noting that a cross section of 0.1 GM has been suggested to be sufficient for biological applications in live specimen samples.[29]

Conclusions

We have prepared a series of photoluminescent Ir(III) and Ru(II) complexes bearing two polar terpyridine ligands. These chromophores have been structurally elaborated from simpler terpyridine derivatives to incorporate a stilbene and ene-anisole moiety by Wittig condensation affording donor–π–acceptor–π–donor assemblies. The solid state structures of representative compounds $[Ir(ttpyeneanisole)_2]\cdot 3PF_6$ and $[Ru(tpystilbene)_2]\cdot 2PF_6$ have been determined; the dihedral angle between the pyridyl and tolyl groups is rather more acute in the Ir(III) complex $[Ir(ttpyeneanisole)_2]\cdot 3PF_6$ and indicates the presence of a greater degree of π-delocalisation across the ttpy unit in this compound than in the Ru(II) derivative. All four complexes exhibit green one-photon photoluminescence when excited in the UV–vis, with relatively large quantum yields in air-equilibrated solutions compared to structurally similar compounds. In both families of complexes, the emission is principally ligand based in origin, and in the case of the Ir(III) complexes $[Ir(ttpyeneanisole)_2]\cdot 3PF_6$ and $[Ir(tpystilbene)_2]\cdot 3PF_6$, the one-photon emission lifetimes are in the microsecond range. All complexes undergo efficient two-photon absorption when excited with a femtosecond titanium sapphire laser in the near infrared, giving rise to luminescence profiles that are analogous to the one-photon emission. The two-photon cross-sections (σ_2), measured as a function of excitation wavelength, correspond well to the one-photon excitation spectra, indicating the emission originates from the same excited states. The Ir(III) complexes in particular show substantial values of σ_2 which suggests that the excited state conformations of the aromatic rings possess a higher degree of co-planarity relative to those in the Ru(II) analogues, thereby affording a higher degree of excited state π-delocalisation. The comparatively high values of σ_2 (evaluated against previously reported metal polypyridyl and acetylide-type compounds) further demonstrates that simple functionalisation of platinum group metal-containing chromophores markedly increases the probability of two-photon absorption, which renders these compounds, or derivatives thereof, suitable candidate dyes for two-photon applications in aerated media. Work towards elucidating the exact nature of the excited states involved in the two-photon processes in tandem with improving the two-photon cross sections and quantum yields of luminescence is currently in progress.

Experimental

General details

All chemical reagents and metal salts were obtained from the Aldrich Chemical Company and were used as supplied. The compounds 4′-(*p*-tolyl)-2,2′:6′,2″-terpyridine,[21] 4′-(phenyl-*p*-bromomethyl)-2,-2′:6′,2″-terpyridine[22] and 4-(2,2′:6′,2″-terpyridyl-4′)-benzyl triphenylphosphonium bromide[17] were prepared according to literature procedures. Reagent grade THF was dried over potassium/benzophenone and distilled prior to use.

Mass spectra were obtained using positive electrospray in acetonitrile or methanol solutions on a Micromass Platform II spectrometer, or by MALDI using methanol solutions with an ALPHA maxtrix on a Micromass TOF Spec 2E spectrometer.

Table 3 Data collection and structural refinement for $[Ir(ttpyeneanisole)_2]\cdot 3PF_6$ and $[Ru(tpystilbene)_2]\cdot 2PF_6$

	$[Ir(ttpyeneanisole)_2]\cdot 3PF_6$	$[Ru(tpystilbene)_2]\cdot 2PF_6$
Diffractometer type	Bruker APEXII CCD	Bruker APEXII CCD
Formula	$C_{60}\ H_{50.67}\ F_{18}\ Ir\ N_6\ O_{4.33}\ P_{3.33}$	$C_{58}\ H_{44}\ F_{12}\ N_6\ O\ P_2\ Ru$
M_r	1600.50	1232.00
Cell setting, space group	Trigonal, $R\bar{3}c$	Orthorhombic, *Pbam*
a, *b*, *c*/Å	25.3220(18), 25.3220(18), 51.3290(18)	15.5722(5), 19.0829(6), 20.3472(7)
α, β, γ (°)	90.00, 90.00, 120.00	90.00, 90.00, 90.00
V/Å^3	28503(3)	6046.4(3)
Z	18	4
D_x/Mg m^{-3}	1.687	1.353
Radiation type	Mo-Kα	Synchrotron
θ range (°)	1.84–23.58	1.96–26.38
μ/mm^{-1}	2.304	0.392
T/K	150(2)	150(2)
R(int)	0.132	0.058
Crystal form, colour	Block, dark red	Block, red
Crystal size/mm	0.10, 0.06, 0.04	0.05, 0.04, 0.02
Data collection method	ϕ and ω	ω with narrow frames
T_{min}	0.8023	0.9807
T_{max}	0.9135	0.9922
No. of measured, independent and observed reflections	9064, 4732, 1914	50953, 6353, 4854
$R[F^2 > 2\sigma(F^2)]$, $wR(F^2)$, S	0.1076, 0.2614, 1.018	0.0652, 0.1987, 1.126
No. of reflections	4732	6353
No. of parameters	423	384
$(\Delta/\sigma)_{max}$	0.002	0.000
$\Delta\rho_{max}$, $\Delta\rho_{min}$/e Å^{-3}	1.388, –0.723	0.807, –0.905

Elemental analyses were performed by the microanalytical services at the University of Manchester using a Carlo ERBA Instruments CHNS–O EA1108 elemental analyzer (C, H, N and S analysis) and a Fisons Horizon Elemental Analysis ICP-OED spectrometer for metals and halogens.

All NMR spectra were recorded on a Bruker Avance 400 spectrometer, operating frequency 400 MHz (^{1}H), 100 MHz (^{13}C), variable temperature unit set at 300 K, unless otherwise stated. Chemical shifts are reported in parts per million relative to TMS and referenced to the residual proton resonances in d_6-DMSO, d_3-acetonitrile, or d_6-acetone. Absorption spectra were recorded in H_2O on a T60U spectrometer (PG Instruments Ltd.) using fused quartz cells with a path length of 1 cm.

X-ray diffraction data for $[Ru(tpystilbene)_2]\cdot 2PF_6$ were collected at 150 K using a Bruker APEX II CCD diffractometer on station 9.8 of the Synchrotron Radiation Source at CCLRC Daresbury Laboratory, at 0.69040 A°, from a silicon 111 monochromator using ω scans. Crystal data, data collection and structural refinement parameters are given in Table 3. The structure was solved by direct methods using the program SHELXS-97.21. The refinement and all further calculations were performed using SHELXL-97.[30] Data were corrected for Lorenz and polarisation factors and an absorption correction applied using Bruker SADABS. The structure was completed by iterative cycles of ΔF-syntheses and a full matrix least square refinement and all non-H atoms were refined anisotropically. Difference Fourier syntheses were employed in positioning idealised hydrogen atoms and were allowed to ride on their parent C or N-atoms. The structure contained

a large number of disordered solvent molecules which could not be modelled and the application of *SQUEEZE*[31] was required. Data for [Ir(ttpyeneanisole)$_2$]·3PF$_6$ were collected on a Nonius κ-CCD four circle diffractometer using graphite-monochromated Mo-Kα radiation at 150 K. Data were corrected for Lorenz and polarisation factors and absorption corrections were applied by the multi-scan method using the SORTAV program.[32]

CCDC reference numbers: 783187 for [Ru(tpystilbene)$_2$]·2PF$_6$ and 783188 for [Ir(ttpyeneanisole)$_2$]·3PF$_6$.

Photophysical characterisation

The quantum yields of luminescence of the complexes were determined relative to quinine sulfate in 0.1 M H_2SO_4, which has a known quantum yield of 58% at 350 nm excitation at 295 K. The details of this approach have been described in detail elsewhere.[33]

Steady state luminescence properties of the ligands and complexes were determined using a PerkinElmer LS50B or LS55 fluorimeter operating in fluorescence mode. Time resolved luminescence measurements of the ligands were recorded using a modified Edinburgh instruments mini-Tau system by time correlated single photon counting using an EPL 405 picosecond diode laser as the excitation source. Lifetimes were obtained by tail fit on the data obtained, and quality of fit judged by minimization of reduced chi-squared and residuals squared. In this modified set-up samples were excited by a pulsed diode laser emitting at 405 nm with a pulse duration of 90 ps. The repetition rate of the laser was set to 2 microseconds to ensure the sample had fully decayed between excitation events. Two 2′ lenses were used to collect the emission and match the f-number of a monochromator (Acton research, SpectraPro 500i). A Hamamatsu H7422 PMT was attached to the output slit of the monochromator which gave an instrument response function with FWHM of ~400 picoseconds. The monochromator was set to 420 or 460 nm corresponding to the emission maxima of the ligands. Time resolved luminescence measurements of the complexes were recorded using an Edinburgh instruments mini-Tau system by time correlated single photon counting using an EPL 375 or EPL 405 picosecond diode laser as the excitation source. Lifetimes were obtained by tail fit on the data obtained, and quality of fit judged by minimization of reduced chi-squared and residuals squared.

Two-photon excitation was performed with a 82 MHz pulsed titanium sapphire laser (Tsunami, Spectra Physics). A portion of the excitation beam was split and detected with a laser spectrum analyser, and the spectrum was monitored continuously to ensure pulse stability (*ca.* 10 nm FWHM). Neutral density filters attenuated the beam, which passed through a dichroic mirror (650DCSPXR, Chroma) and was focused with a 40× objective (PF, NA = 0.60, Nikon) onto the sample, which was in a 1 cm pathlength cuvette. The incident power was monitored throughout (Uno meter and PH100-Si head, Gentech). The sample fluorescence was collected by the same objective and reflected from the dichroic mirror, passed through a shortpass filter (HQ 575/150, Chroma) to remove residual excitation light and detected by a fibre-coupled spectrometer (Ocean Optics QE65000).

The two-photon cross sections, σ_2, were measured by recording spectra of the complexes in MeCN (*ca.* 10^{-4} M) and comparing them to that of a standard, rhodamine B in methanol, as described previously using eqn (1).[10]

$$\frac{\sigma_2^S \phi^S}{\sigma_2^R \phi^R} = \frac{\eta^R n^S C^R F^S P^R}{\eta^S n^R C^S F^R P^S} \quad (1)$$

where ϕ is the quantum yield of fluorescence, η is a term that accounts for the wavelength-dependent collection efficiency of the fluorescence (due to the reflectance/transmission of the various optical components and the sensitivity of the detector), n is the refractive index of the solvent, C is the concentration, F is the integrated fluorescence signal from the recorded spectrum, P is the excitation power, and S and R refer to sample and reference, respectively. The sample and reference were always recorded under identical conditions on the same day, so the P terms cancel. We have also omitted the η terms due to the similarity in spectra for sample and reference, which should not introduce a significant error. For ϕ^S, we use the quantum yields measured for the complexes under one-photon conditions (Table 1). For rhodamine B in methanol, we have used the wavelength-dependent values of σ_2 reported recently[34] and a value of $\phi^R = 0.7$.[35] We estimate an experimental precision of ± 30%. The experimental setup was verified by observing the expected quadratic dependence of fluorescence of rhodamine B in methanol on excitation intensity.

Synthesis of ligands and complexes

Preparation of 4-(4-{2-[4-(methoxy)phenyl]ethenyl}phenyl)-2,2′-6′,2″-terpyridine (ttpyeneanisole). Under N_2, a flamed out Schlenk flask was loaded with 4-(2,2′:6′,2″-terpyridyl-4′)-benzyl triphenylphosphonium bromide (1.2 g, 1.81 mmol) and potassium *tert*-butoxide (1.46 g, 7.24 mmol). The flask was immersed in an ice bath and 40 mL dry THF added by cannula; the solution was stirred at 0 °C for 30 min during which time the solution turned bright orange. 0.246 g (1.81 mmol) *p*-anisaldehyde was then added dropwise over 20 min and the solution slowly warmed to room temperature and stirred for a further 72 h. After this time, the reaction was quenched by the addition of ice water, and all solvents removed under reduced pressure. Methanol was added to the residue (60 mL) and the solution stirred overnight at room temperature. The precipitated yellow solid was isolated by vacuum filtration, washed with water (3 × 10 mL), methanol (5 × 10 mL) and diethylether (3 × 10 mL) to afford a pale yellow solid that exhibits limited solubility in $CHCl_3$ and DMSO, 0.39 g, 49%.

MALDI MS (alpha): m/z 452 $\{M + H\}^+$ (100%). NMR/$CDCl_3$ δ_H: 8.68 (s, H_3', H_5'), 8.67 (dd, $^3J_{HH}$ 4.0 Hz, $^4J_{HH}$ 1.6 Hz, H_6, H_6'') (overlapping signals, 4H), 8.61 (d, 2H, $^3J_{HH}$ 8.0 Hz, H_3, H_3''), 7.85 (d, $^3J_{HH}$ 8.4 Hz, H_7, H_7'), 7.82 (td, $^3J_{HH}$ 8.4 Hz, $^4J_{HH}$ 1.6 Hz, H_4, H_4'') (overlapping signals, 4H), 7.56 (d, 2H, $^3J_{HH}$ 8.4 Hz, H_8, H_8''), 7.43 (d, 2H, $^3J_{HH}$ 8.8 Hz, H_{14}, H_{14}'), 7.23 (m, 2H, H_5, H_5''), 7.10 (d, 1H, $^2J_{HH}$ 16.4 Hz, H_{10}/H_{11}), 6.97 (d, 1H, $^2J_{HH}$ 16.4 Hz, H_{10}/H_{11}), 6.85 (d, 2H, $^3J_{HH}$ 8.4 Hz, H_{13}, H_{13}'), 3.78 (s, 3H, OMe). UV–vis (DMSO) λ_{max} (ε/mol^{-1}dm^{3}cm) = 287 (30400), 352 (42500). Anal. Calcd. For $C_{30}H_{23}N_3O$: C 81.61, H 5.25, N 9.52. Found: C 81.32, H 5.31, N 9.41.

Preparation of 4-(4-{2-[phenyl]ethenyl}phenyl)-2,2′-6′,2″-terpyridine (tpystilbene). Under N_2, a flamed out Schlenk flask was loaded with 4-(2,2′:6′,2″-terpyridyl-4′)-benzyl triphenylphosphonium bromide (0.8 g, 1.21 mmol) and potassium *tert*-butoxide (0.97 g, 4.83 mmol). The flask was immersed in an ice bath and 40 mL dry THF added by cannula; the solution was stirred at 0 °C for 30 min during which time the

solution turned bright orange. 0.128 g (1.21 mmol) benzaldehyde was then added dropwise over 20 min and the solution slowly warmed to room temperature and stirred for a further 24 h. After this time, the reaction was quenched by the addition of ice water, and all solvents removed under reduced pressure. The product was extracted into CH_2Cl_2, and washed with H_2O and brine. The organic layer was dried over $MgSO_4$ and all volatiles were removed under reduced pressure. Methanol was added to the solid (40 mL) and the solution stirred overnight hours at room temperature. The precipitated solid was isolated by vacuum filtration, washed with methanol (5 × 10 mL) and diethylether (3 × 10 mL) to afford a white powder, 0.19 g, 39%.

MALDI MS (alpha): m/z 411 $\{M + H\}^+$ (100%). NMR/$CDCl_3$ δ_H: 8.77 (s, H_3', H_5'), 8.75 (d, $^3J_{HH}$ 4.0 Hz, H_6, H_6'') (overlapping signals, 4H), 8.68 (d, 2H, $^3J_{HH}$ 8.0 Hz, H_3, H_3''), 7.93 (d, $^3J_{HH}$ 8.4 Hz, H_7, H_7'), 7.90 (td, $^3J_{HH}$ 8.0 Hz, $^4J_{HH}$ 1.6 Hz, H_4, H_4'') (overlapping signals, 4H), 7.66 (d, 2H, $^3J_{HH}$ 8.0 Hz, H_8, H_8''), 7.56 (d, 2H, $^3J_{HH}$ 7.2 Hz, H_{14}, H_{14}'), 7.36 (m, 4H, H_5, H_5'', H_{10}, H_{11}), 7.30 (t, 1H, $^3J_{HH}$ 7.2 Hz, H_{15}), 7.20 (d, 2H, $^3J_{HH}$ 5.6 Hz, H_{13}, H_{13}'). δ_C: 156.29, 155.98, 149.70, 138.15, 137.43, 137.18 (quarternary C_2, C_2'', C_2', C_6', C_6, C_9, C_{12}), 149.16 (C_3', C_5'), 136.90 (C_6, C_6''), 129.55 (C_{14}, C_{14}'), 128.00, 128.75, 127.85, 123.86 (C_5, C_5'' C_{10}, C_{11}, C_{15}), 127.62 (C_7, C_7'), 127.05 (C_8, C_8'), 126.65 (C_{13}, C_{13}'), 121.40 (C_3, C_3''), 118.55 (C_6, C_6''). UV–vis (DMSO) λ_{max} (ε/mol^{-1}dm^{3}cm) = 289 (27700), 336 (46200). Anal. Calcd. For $C_{29}H_{21}N_3$: C 84.64, H 5.14, N 10.21. Found: C 84.50, H 4.81, N 10.15.

Preparation of ruthenium bis{4-(4-{2-[4-(methoxy)phenyl]-ethenyl}-phenyl)-2,2′-6′,2″-terpyridine}·2PF$_6$ ([Ru(ttpyeneanisole)$_2$]·2PF$_6$). Under N_2, an ethanolic solution of $RuCl_3 \cdot xH_2O$ (0.071 g, 15 mL) and ttpyeneanisole (0.10 g, 0.226 mmol) was heated to reflux temperature for 15 h. After this time, the precipitated solid was isolated by filtration, washed with H_2O (2 × 5 mL), EtOH (5 × 5 mL) and CH_2Cl_2 (2 × 5 mL) then dried to yield 0.124 g of Ru(ttpyeneanisole)·Cl_3 as an insoluble red–brown powder (85% based on ttpyeneanisole). In the dark and under N_2, 0.078 g AgOTf (0.303 mmol) was then added to a slurry of Ru(ttpyeneanisole)·Cl_3 (0.050 g, 0.087 mmol) in 15 mL EtOH–acetone (1 : 4 v:v). The solution was then heated at reflux temperature for 24 h. The red solution was subsequently filtered through a pad of celite, and all volatiles removed under reduced pressure. The residue was dissolved in 12 mL EtOH and 0.038 g (0.087 mmol) ttpyeneanisole added as a solid. The resultant slurry was heated to reflux temperature for 3 days (or until all the terpyridine ligand had been consumed), then all volatiles were removed by rotary evaporation. 15 mL methanol was added to the red solid, the solution filtered through a pad of celite and a saturated aqueous solution of NH_4PF_6 added to precipitate the product as the PF_6 salt. The precipitated solid was isolated by filtration and recrystallised three times from MeCN–Et_2O to afford 0.052 g of [Ru(tpystilbene)$_2$]·3PF_6 as a red powder in 47% yield.

ES$^+$ MS (MeCN) m/z 1130 $\{M - PF_6\}^+$ (6%), 492 $\{M - 2 \times PF_6\}^{2+}$ (100%). NMR/d_6-acetone δ_H: 9.36 (s, 4H, H_3', H_5'), 8.96 (d, 4H, 8.0 Hz, H_6, H_6''), 8.25 (d, 4H, $^3J_{HH}$ 8.4 Hz, H_7, H_7''), 7.99 (td, 4H, $^3J_{HH}$ 8.0 Hz, $^4J_{HH}$ 1.6 Hz H_4, H_4'), 7.84 (d, 4H, $^3J_{HH}$ 8.4 Hz, H_8, H_8''), 7.73 (dd, 2H, $^3J_{HH}$ 5.6 Hz, $^4J_{HH}$ 0.8 Hz, H_3, H_3''), 7.52 (d, 4H, $^3J_{HH}$ 8.8 Hz, H_{14}, H_{14}'), 7.35 (d, 2H, $^2J_{HH}$ 16.4 Hz, H_{10}/H_{11}), 7.24 (m, 4H, H_5, H_5''), 6.97 (d, 2H, $^2J_{HH}$ 16.4 Hz, H_{10}/H_{11}), 6.89 (d, 2H, $^3J_{HH}$ 8.4 Hz, H_{13}, H_{13}'), 3.74 (s, 6H, OMe). UV–vis (MeCN) λ_{max} (ε/mol^{-1}dm^{3}cm) = 233 (sh), (37600), 287 (sh), (45000), 310 (61200), 328 (sh), (52300), 357 (42500), 497 (35600). Accurate Mass ES$^+$ MS (MeCN): composition $C_{60}H_{46}N_6O_2Ru_1$, theoretical 492.1357, measured 492.1355, error 0.5 ppm.

Preparation of ruthenium bis{4-(4-{2-[phenyl]ethenyl}-phenyl)-2,2′-6′,2″-terpyridine}·2PF$_6$ ([Ru(tpystilbene)$_2$]·2PF$_6$). Under N_2, an ethanolic solution of $RuCl_3 \cdot xH_2O$ (0.064 g, 10 mL) and tpystilbene (0.070 g, 0.171 mmol) was heated to reflux temperature for 15 h. After this time, the precipitated solid was isolated by filtration, washed with H_2O (2 × 5 mL), EtOH (5 × 5 mL) and CH_2Cl_2 (2 × 5 mL) then dried to yield 0.11 g of Ru(tpystilbene)·Cl_3 as an insoluble red–brown powder (87% based on tpystilbene). In the dark and under N_2, 0.073 g AgOTf (0.283 mmol) was then added to a slurry of Ru(tpystilbene)·Cl_3 (0.050 g, 0.081 mmol) in 12 mL EtOH–acetone (1 : 4 v:v). The solution was then heated at reflux temperature for 24 h. The red solution was subsequently filtered through a pad of celite, and all volatiles removed under reduced pressure. The residue was dissolved in 10 mL EtOH and 0.033 g tpystilbene (0.081 mmol) added as a solid. The resultant slurry was heated to reflux temperature for 3 days (or until all the terpyridine ligand had been consumed), then all volatiles were removed by rotary evaporation. 15 mL methanol was added to the red solid, the solution filtered through a pad of celite and a saturated aqueous solution of NH_4PF_6 added to precipitate the product as the PF_6 salt. The precipitated solid was isolated by filtration and recrystallised three times from MeCN–Et_2O to afford 0.046 g of Ru(tpystilbene)$_2$·3PF_6 as a red powder in 51% yield. Single crystals were grown from slow evaporation of a concentrated acetone solution at room temperature.

ES$^+$ MS (MeCN) m/z 1069 $\{M - PF_6\}^+$ (4%), 462 $\{M - 2 \times PF_6\}^{2+}$ (100%). NMR/d_6-acetone δ_H: 9.38 (s, 4H, H_3', H_5'), 8.98 (d, 4H, $^3J_{HH}$ 8.0 Hz, H_6, H_6''), 8.29 (d, 4H, $^3J_{HH}$ 8.4 Hz, H_7, H_7''), 7.99 (td, 4H, $^3J_{HH}$ 8.0 Hz, $^4J_{HH}$ 1.2 Hz H_4, H_4'), 7.88 (d, 4H, $^3J_{HH}$ 8.4 Hz, H_8, H_8''), 7.73 (d, 2H, $^3J_{HH}$ 5.2 Hz, H_3, H_3''), 7.58 (d, 4H, $^3J_{HH}$ 7.2 Hz, H_{14}, H_{14}'), 7.40 (d, 2H, $^2J_{HH}$ 16.4 Hz, H_{10}/H_{11}), 7.30 (m, 8H, H_{10}/H_{11}, H_5, H_5''), 7.24 (m, 6H, H_{13}, H_{13}', H_{15}). UV–vis (MeCN) λ_{max} (ε/mol^{-1}dm^{3}cm) = 223 (sh), (31600), 274 (sh), (24300), 287 (sh) (30900), 312 (47600), 335 (47600), 353 (48000), 496 (28400). Accurate Mass ES$^+$ MS (MeCN): composition $C_{58}H_{42}N_6Ru_1$, theoretical 461.6201, measured 461.6196, error 1.0 ppm.

Preparation of iridium bis{4-(4-{2-[4-(methoxy)phenyl]-ethenyl}-phenyl)-2,2′-6′,2″-terpyridine}·3PF$_6$ ([Ir(ttpyeneanisole)$_2$]·3PF$_6$). According to a modification of a literature procedure,[24,25] under N_2, a mixture of $IrCl_3 \cdot xH_2O$ (0.050 g, 0.167 mmol) and ttpyeneanisole (0.148 g, 0.335 mmol) in ethylene glycol (12 mL) was heated at 100 °C for 2.5 h. After this time, the temperature was raised to 195 °C and the reaction mixture maintained at this temperature for a further 1.5 h. The dark red solution was cooled and added to a saturated solution of NH_4PF_6 to precipitate the complex as the PF_6 salt. The dark red precipitate was isolated by vacuum filtration and washed with H_2O (3 × 5 mL), MeOH (3 × 5 mL) and Et_2O (3 × 5 mL). Repeated recrystallisation (3–5 times) from MeCN–Et_2O afforded dark red crystals of [Ir(ttpyeneanisole)$_2$]·3PF_6 in 53% yield (0.121 g).

ES$^+$ MS (MeCN) m/z 1366 $\{M - PF_6\}^+$ (8%), 610 $\{M - 2 \times PF_6\}^{2+}$ (34%), 358 $\{M - 3 \times PF_6\}^{3+}$ (100%). NMR/d_6-acetone δ_H: 9.57 (s, 4H, H_3', H_5'), 9.17 (d, 4H, 8.0 Hz, H_6, H_6''), 8.37 (td,

$^3J_{HH}$ 8.0 Hz, $^4J_{HH}$ 1.2 Hz H_4, H_4'), 8.34 (d, $^3J_{HH}$ 8.0 Hz, H_7, H_7'') (overlapping signals, 8H), 8.24 (dd, $^3J_{HH}$ 6.0 Hz, $^4J_{HH}$ 0.8 Hz, H_3, H_3''), 7.94 (d, 4H, $^3J_{HH}$ 8.4 Hz, H_8, H_8''), 7.62 (m, 8H, H_5, H_5'', H_{14}, H_{14}''), 7.47 (d, 2H, $^2J_{HH}$ 16.4 Hz, H_{10}/H_{11}), 7.27 (d, 4H, H_{10}/H_{11}), 6.97 (d, 4H, $^3J_{HH}$ 8.8 Hz, H_{13}, H_{13}'), 3.81 (s, 6H, OMe). UV–vis (MeCN) λ_{max} (ε/mol^{-1}dm^{3}cm) = 222 (sh), (55640), 250 (48830), 323 (77100), 434 (40180). Anal. Calcd. For $C_{60}H_{46}N_6O_2P_3F_{18}Ir{\cdot}2H_2O$: C 46.61, H 3.26, N 5.44. Found: C 46.81, H 3.25, N 5.24.

Preparation of iridium bis{4-(4-{2-[phenyl]ethenyl}-phenyl)-2,2′-6′,2″-terpyridine}·3PF$_6$ ([Ir(tpystilbene)$_2$]·3PF$_6$). Under N_2, a mixture of $IrCl_3{\cdot}xH_2O$ (0.022 g, 0.075 mmol) and tpystilbene (0.050 g, 0.147 mmol) in ethylene glycol (7 mL) was heated at 100 °C for 2.5 h. After this time, the temperature was raised to 195 °C and the reaction mixture maintained at this temperature for a further 1.5 h. The dark orange solution was cooled and added to a saturated solution of NH_4PF_6 to precipitate the complex as the PF_6 salt. The orange precipitate was isolated by vacuum filtration and washed with H_2O (3 × 5 mL), MeOH (3 × 5 mL) and Et_2O (3 × 5 mL). Repeated recrystallisation (4–5 times) from acetone–Et_2O afforded an orange powder of [Ir(tpystilbene)$_2$]·3PF$_6$ in 34% yield (0.036 g).

ES$^+$ MS (MeCN) m/z 1305 {M – PF$_6$}$^+$ (9%), 1159 {M – 2 × PF$_6$ + H}$^+$ (6%), 508 {M – 2 × PF$_6$}$^+$ (54%), 339 {M – 3 × PF$_6$}$^{3+}$ (100%). NMR/d_6-acetone δ_H: 9.45 (s, 4H, H_3', H_5'), 9.06 (d, 4H, $^3J_{HH}$ 7.2 Hz, H_6, H_6''), 8.26 (d, 4H, $^3J_{HH}$ 8.0 Hz, H_7, H_7''), 8.14 (m, 4H, H_4, H_4'), 7.91 (d, 4H, $^3J_{HH}$ 8.0 Hz, H_8, H_8''), 7.58 (d, 4H, H_{14}, H_{14}'), 7.48 (m, 8H, H_3, H_3'', H_5, H_5''), 7.34 (m, 6H, H_{10}, H_{11}, H_{15}), 6.74 (d, 4H, $^3J_{HH}$ 7.6 Hz, H_{13}, H_{13}'). UV–vis (MeCN) λ_{max} (ε/mol^{-1}dm^{3}cm) = 252, (56580), 292 (63360), 320 (sh) (56030), 377 (29240). Anal. Calcd. For $C_{58}H_{42}N_6P_3F_{18}Ir{\cdot}2H_2O$: C 46.87, H 3.12, N 5.65. Found: C 46.44, H 2.78, N 5.58.

Acknowledgements

We thank the EPSRC for funding a Career Acceleration Fellowship (LSN) and an Advanced Research Fellowship (SWM) and The Leverhulme Trust for a postdoctoral fellowship (LSN). We also thank Dr Alisdair Macpherson for his assistance with the titanium sapphire laser, Dr David Binks and Dr Stuart Stubbs for help with the lifetime measurements of the uncomplexed ligands and Dr Robin Pritchard and Dr Rachel Shaw for the X-ray crystallographic data collection of [Ir(ttpyeneanisole)$_2$]·3PF$_6$ and [Ru(tpystilbene)$_2$]·2PF$_6$ respectively.

Notes and references

1 For recent comprehensive reviews of two photon materials and their technological applications, see: G. S. He, L.-S. Tan, Q. Zheng and P. N. Prasad, *Chem. Rev.*, 2008, **108**, 1245; H. M. Kim and B. R. Cho, *Chem. Commun.*, 2009, 153; H. M. Kim and B. R. Cho, *Acc. Chem. Res.*, 2009, **42**, 863; F. Helmchen and W. Denk, *Nature*, 2005, **2**, 932; M. Pawlicki, H. A. Collins, R. G. Denning and H. L. Anderson, *Angew. Chem., Int. Ed.*, 2009, **48**, 3244.

2 G. S. He, P. P. Marcowicz, T.-C. Lin and P. N. Prasad, *Nature*, 2002, **415**, 767.

3 C. C. Corredor, Z.-L. Huang and K. D. Belfield, *Adv. Mater.*, 2006, **18**, 2910; C. C. Corredor, Z.-L. Huang, K. D. Belfield, A. R. Morales and M. V. Bondar, *Chem. Mater.*, 2007, **19**, 5165; A. S. Dvornikov, E. P. Walker and P. M. Rentzepis, *J. Phys. Chem. A*, 2009, **113**, 13633; E. Walker, A. Dvornikov, K. Coblentz and P. Renzepis, *Appl. Optics*, 2008, **47**, 4130.

4 C. Giradot, B. Cao, J.-C. Mulatier, P. L. Baldeck, J. Chauvin, D. Riehl, J. A. Delaire, C. Andraud and G. Lemercier, *ChemPhysChem*, 2008, **9**, 1531; E. Glimsdal, M. Carlsson, T. Kindahl, M. Lindgren, C. Lopes and B. Eliasson, *J. Phys. Chem. A*, 2010, **114**, 3431.

5 S. Maruo, O. Nakamura and S. Kawata, *Opt. Lett.*, 1997, **22**, 132; C. N. LaFratta, J. T. Fourkas, T. Baldacchini and R. A. Farrer, *Angew. Chem., Int. Ed.*, 2007, **46**, 6238.

6 A. Zoumi, A. Yeh and B. J. Tromberg, *Proc. Natl. Acad. Sci. U. S. A.*, 2002, **99**, 11014; M. D. Cahalan, I. Parker, S. H. Wei and M. J. Miller, *Nature*, **2**, 872; W. Denk, J. H. Strickler and W. W. Webb, *Science*, 1990, **248**, 73; N. J. Durr, T. Larson, D. K. Smith, B. A. Korgel, K. Sokolov and A. Ben-Yakar, *Nano Lett.*, 2007, **7**, 941; D. J. S. Birch, *Spectrochim. Acta, Part A*, 2001, **57**, 2313.

7 J. Arnbjerg, A. Jiménez-Banzo, M. J. Paterson, S. Nonell, J. I. Borrell, O. Christiansen and P. R. Ogilby, *J. Am. Chem. Soc.*, 2007, **129**, 5188; J. P. Celli, B. Q. Spring, I. Rizvi, C. L. Evans, K. S. Samkoe, S. Verma, B. W. Pogue and T. Hasan, *Chem. Rev.*, 2010, **110**, 2831; J. R. Starkey, A. K. Rebane, M. A. Drobizhev, F. Meng, A. Gong, A. Elliot, K. McInnerney and C. W. Spangler, *Clin. Cancer Res.*, 2008, **14**, 6564.

8 A. Momotake, N. Lindegger, E. Niggli, R. J. Barsotti and G. C. R. Llis-Davies, *Nat. Methods*, 2006, **3**, 35; H. Lusic, R. Uprety and A. Deiters, *Org. Lett.*, 2010, **12**, 916; A. P. Goodwin, J. L. Mynar, Y. Ma, G. R. Fleming and J. M. Fréchet, *J. Am. Chem. Soc.*, 2005, **127**, 9952.

9 W. R. Zipfel, R. M. Williams and W. W. Webb, *Nat. Biotechnol.*, 2003, **21**, 1369.

10 M. H. V. Werts, N. Nerambourg, D. Pélégry, Y. LeGrand and M. Blanchard-Desce, *Photochem. Photobiol. Sci.*, 2005, **4**, 531.

11 J. E. Ehrlich, X. L. Wu, I.-Y. S. Lee, Z.-Y. Hu, H. Röckel, S. R. Marder and J. W. Perry, *Opt. Lett.*, 1997, **22**, 1843; M. Albota, D. Beljonne, J.-L. Brédas, J. E. Ehrlich, J.-Y. Fu, A. A. Heikal, S. E. hess, T. Kogej, M. D. Levin, S. R. Marder, O. McCord-Maughon, J. W. Perry, H. Röckel, M. Rumi, G. Subramaniam, W. W. Webb, X.-L. Wu and C. Xu, *Science*, 1998, **281**, 1653; B. A. Reinhardt, L L. Brott, S. J. Clarson, A. G. Dillard, J. C. Bhatt, R. Kannan, L. Yuan, G. S. He and P. N. Prasad, *Chem. Mater.*, 1998, **10**, 1863; H. M. Kim, M. S. Seo, S.-J. Jeon and B. R. Cho, *Chem. Commun.*, 2009, 7422.

12 S. W. Botchway, M. Charnley, J. W. Haycock, A. W. Parker, D. L. Rochester, J. A. Weinstein and J. A. G. Williams, *Proc. Natl. Acad. Sci. U. S. A.*, 2008, **105**, 16071; T. J. McKay, J. Staromlynska, P. Wilson and J. Davy, *J. Appl. Phys.*, 1999, **85**, 1337; Z.-D. Yang, J.-K. Feng and A.-M. Ren, *Inorg. Chem.*, 2008, **47**, 10841; C.-K. Koo, K. = L. Wong, C. W.-Y. Man, Y.-W. Lam, L. K.-Y. So, H.-L. Tam, S.-W. Tsao, K.-W. Cheah, K.-C. Lau, Y.-Y. Yang, J.-C. Chen and M. H.-W. Lam, *Inorg. Chem.*, 2009, **48**, 872; C.-H. Tao, H. Yang, N. Zhu, V. W.-W. Yam and S.-J. Xu, *Organometallics*, 2008, 5453; C. K. M. Chan, C.-H. Tao, H.-L. Tam, N. Zhu, V. W.-W. Yam and K.-W. Cheah, *Inorg. Chem.*, 2009, **48**, 2855; C.-H. Tao and V. W.-W. Yam, *J. Photochem. Photobiol., C*, 2009, **10**, 130.

13 A. M. McDonagh, M. G. Humphry, M. Samoc, B. Luther-Davies, S. Houbrechts, T. Wada, H. sasabe and A. Persoons, *J. Am. Chem. Soc.*, 1999, **121**, 1405; C. Feuvrie, O. Maury, H. Le Bozec, I. Ledoux, J. P. Morrall, G. T. Dalton, M. Samoc and M. G. Humphrey, *J. Phys. Chem. A*, 2007, **111**, 8980; C. Giradot, G. Lemercier, J.-C. Mulatier, J. Chauvin, P. L. Baldeck and C. Andraud, *Dalton Trans.*, 2007, 3421; L. Yang, X.-H. Zhao, H.-P. Zhou, J.-Y. Wu, J.-X. yang, G.-Q. Shao and Y.-P. Tian, *Transition Met. Chem.*, 2008, **33**, 431.

14 Y. Sekiguchi, T. Yamashita and M. Vacha, *J. Luminescence*, 2008, **128**, 848; Y. Koide, S. Takahashi and M. Vacha, *J. Am. Chem. Soc.*, 2006, **128**, 10990.

15 A. Picot, F. Maltovi, B. Le Guennic, P. L. Baldeck, J. A. G. Williams, C. Andraud and O. Maury, *Inorg. Chem.*, 2007, **46**, 2659; L.-M. Fu, X.-F. Wen, X.-C. Ai, Y. Sun, Y.-S. Wu, J.-P. Zhang and Y. Wang, *Angew. Chem., Int. Ed.*, 2005, **44**, 747; K.-L. Wong, W.-M. Kwok, W.-T. Wong, D. L. Phillips and K.-W. Cheah, *Angew. Chem., Int. Ed.*, 2004, **43**, 4659; L.-O. Pålsson, R. Pal, B. S. Murray, D. Parker and A. Beeby, *Dalton Trans.*, 2007, 5726; Filip Kielar, A. Congreve, G. Law, E. J. New, D. Parker, K.-L. Wong, P. Casstreño and J. de Mendoza, *Chem. Commun.*, 2008, 2435; M. H. V. Werts, N. Nerambourg, D. Pélégry, Y. Le Grand and M. Blanchard-Desce, *Photochem. Photobiol. Sci.*, 2005, **4**, 531.

16 X.-B. Zhang, J.-K. Feng and A.-M. Ren, *J. Phys. Chem. A*, 2007, **111**, 1328.

17 F. Tessore, D. Roberto, R. Ugo, M. Pizzotti, S. Quici, M. Cavazzini and S. Bruni, *Inorg. Chem.*, 2005, **44**, 8967.

18 B. J. Coe, *Acc. Chem. Res.*, 2006, **39**, 383; B. J. Coe, M. Samoc, A. Samoc, L. Zhu, Y. Yi and Z. Shuai, *J. Phys. Chem. A*, 2007, **111**, 472;

C. Dragonetti, S. Righetto, D. Roberto, R. Ugo, A. Valore, S. Fantacci, A. Sgamelloti and F. De Angelis, *Chem. Commun.*, 2007, 4116; M. Samoc, G. T. Dalton, J. A. Gladysz, Q. Zheng, Y. Velkov, H. Agren, P. Norman and M. G. Humphrey, *Inorg. Chem.*, 2008, **47**, 9946; M. Konstantaki, E. Koudoumas, S. Couris, P. Laine, E. Amouyal and S. Leach, *J. Phys. Chem. B*, 2001, **105**, 10797; A. Scarpaci, C. Monnerau, N. Hergué, E. Blart, S. Legoupy, F. Obodel, A. Gorfo, J. Pérez-Moreno and I. Asselberghs, *Dalton Trans.*, 2009, 4538.

19 A. I. Bata, J. R. Shaw, J. A. Simon, R. P. Thummel and R. H. Schmehl, *Coord. Chem. Rev.*, 1998, **171**, 43; Y. You, J. Seo, S. H. Kim, K. S Kim, T. K. Ahn, D. Kim and S. Y. Park, *Inorg. Chem.*, 2008, **47**, 1476; P. Coppo, M. Duati, V. N. Kozhevnikov, J. W. Hofstraat and L. De Cola, *Angew. Chem., Int. Ed.*, 2005, **44**, 1806; K. Y. Zhang and K. K.-W. Lo, *Inorg. Chem.*, 2009, **48**, 6011; C.-J. Chang, C.-H. Yang, K. Chen, Y. Chi, C.-F. Shu, M.-L. Ho, Y.-S. Yeh and P.-T. Chou, *Dalton Trans.*, 2007, 1881.

20 A. Beeby, S. W. Botchway, I. M. Clarkson, S. Faulkner, A. W. Parker, D. Parker and J. A. G. Williams, *J. Photochem. Photobiol., B*, 2000, **57**, 83.

21 D. Roberto, F. Tessore, R. Ugo, S. Bruni, A. Manfred and S. Quinci, *Chem. Commun.*, 2002, 846.

22 W. Spahni and G. Calzaferri, *Helv. Chim. Acta*, 1984, **67**, 450.

23 M. Maestri, N. Armaroli, V. Balzani, E. C. Constable and A. M. W. Cargill Thompson, *Inorg. Chem.*, 1995, **34**, 2759.

24 W. Leslie, A. S. Batsanov, J. A. K. Howard and J. A. G. Williams, *Dalton Trans.*, 2004, 623.

25 J.-P. Collin, I. M. Dixon, J.-P. Sauvage, J. A. G. Williams, F. Barigelletti and L. Flamigni, *J. Am. Chem. Soc.*, 1999, **121**, 5009; J. A. G. Williams, A. J. Wilkinson and V. L. Whittle, *Dalton Trans.*, 2008, 2081; L. Flamigni, A. Barberi, C. Sabatini, B. Ventura and F. Barigelletti, *Top. Curr. Chem.*, 2007, **281**, 143.

26 K. Lashgari, M. Kritikos, R. Norrestam and T. Norby, *Acta Crystallogr., Sect. C: Cryst. Struct. Commun.*, 1999, **C55**, 64; B. Schulze, C. Friebe, M. D. Hager, A. Winter, R. Hoogenboom, H. Görls and U. S. Schubert, *Dalton Trans.*, 787; D. Chartrand, I. Theobold and G. S. Hanan, *Acta Crystallogr., Sect. E: Struct. Rep. Online*, 2007, **63**, 1561; C. Bhaumik, S. Das, D. Saha, S. Dutta and S. Baitalik, *Inorg. Chem.*, 2010, **49**, 5049.

27 H.-Y. Ding, X-S. Wang, L.-Q. Song, J.-R. Chen, J.-H. Yu, C. -Li and B.-W. Zhang, *J. Photochem. Photobiol., A*, 2006, **177**, 286.

28 E. A. Medylcott and G. S. Hanan, *Chem. Soc. Rev.*, 2005, **34**, 133; E. C. Constable, *Chem. Soc. Rev.*, 2007, **36**, 246; J.-P. Sauvage, J.-P. Collin, J.-C. Chambron, S. Guillerez, C. Coudret, V. Balzani, F. Barigelletti, L. De Cola and F. Flamigni, *Chem. Rev.*, 1994, **94**, 993.

29 T. Furuta, S. S.-H. Wang, J. L. Dantzker, T. M. Dore, V. J. Bybee, E. M. Callaway, W. Denk and R. Y. Tsien, *Proc. Natl. Acad. Sci. U. S. A.*, 1999, **96**, 1193.

30 G. M. Sheldrick, *SHELXTL 5.04*, An integrated system for solving, refining and displaying crystal structures from diffraction data, Siemens Analytical X-ray Instruments Inc., Madison, WI, 1995; PLATON,; A. L. Speck, *Acta Crystallogr. Sect. A*, 1990, **46**, C34.

31 SQUEEZE, P. v. d. Sluis and A. L. Speck, *Acta Crystallogr., Sect. A: Found. Crystallogr.*, 1990, **46**, 194.

32 R. H. Blessing, *Acta Crystallogr.*, 1997, **30**, 563.

33 I. M. Clarkson, A. Beeby, J. I. Bruce, J. L. Govenlock, M. P Lowe, C. E. Mathieu, D. Parker and K. Senanayake, *New J. Chem.*, 2000, **24**, 377; R. A. Poole, G. Bobba, M. J. Cann, J.-C. Frias, D. Parker and R. Peacock, *Org. Biomol. Chem.*, 2005, **3**, 1013.

34 N. S. Makarov, M. Drobizhev and A. Rebane, *Opt. Express*, 2008, **16**, 4029.

35 J. N. Demas and G. A. Crosby, *J. Phys. Chem.*, 1971, **75**, 991.

